Methanethiol Chemisorption on Cu(110): Chemical and Geometrical Issues Related to Self-Assembly

Jae-Gook Lee and John T. Yates, Jr.*

Surface Science Center, Department of Chemistry, University of Pittsburgh, Pittsburgh, Pennsylvania 15260

Received: February 26, 2003; In Final Form: July 8, 2003

The adsorption of methanethiol on the clean Cu(110) and the sulfur-passivated Cu(110) surface has been studied with the time-of-flight electron-stimulated desorption ion angular distribution (TOF-ESDIAD) method, temperature-programmed desorption (TPD), and low-energy electron diffraction (LEED). Methanethiol on the clean Cu(110) surface thermally decomposes below 320 K, producing CH_4(g) and C_2H_6(g), leaving the sulfur atom on the surface. A $c(2 \times 2)$ LEED pattern was observed at a low coverage of sulfur, and a $c(8 \times 2)$ structure developed from the $c(2 \times 2)$ phase at the saturation coverage of sulfur. Chemisorbed sulfur acts as a poison for further methanethiol decomposition on the surface. On the sulfur-passivated Cu(110) surface, methanethiol adsorbs dissociatively and produces a methanethiolate layer on the surface. The molecular orientation of CD_3S on the sulfur-passivated Cu(110) surface was determined by assessing the C−D bond direction with respect to the surface normal and the crystal azimuths using the TOF-ESDIAD method. The C−S bond direction in the methanethiolate on the sulfur-passivated Cu(110) surface was oriented parallel to the ⟨001⟩ azimuthal plane. The C−S bond axis of methanethiolate is tilted 45° away from the surface normal.

1. Introduction

The study of the adsorption and thermal decomposition of sulfur-containing compounds on transition metals has been motivated by the need to know the mechanisms involved in desulfurization catalysts and catalytic poisoning by sulfur in industrial processes.[1−5] Additionally, the adsorption of alkanethiols on metal surfaces has attracted much attention because of the scientific and technological importance of self-assembled monolayers (SAMs) made from thiolate species. These SAMs can be used to modify the chemical and physical properties of surfaces for applications such as wetting modification, lubrication, sensors, and corrosion prevention.[6−11]

Alkanethiol molecules form well-ordered layers on Au and Ag surface. While on Au the existence of the intact RS−H bond is currently controversial, on atomically clean Ag definite evidence against the scission of the $CH_3S\cdots H$ bond has recently been found.[12] Many studies related to adsorption and decomposition of CH_3SH on various transition metal surfaces have been carried out since CH_3SH is the simplest alkanethiol. However, the adsorption geometry and decomposition of methanethiol on copper surfaces are not completely understood.

Chemisorbed methanethiolate formed through deprotonation can occupy various surface sites and exhibit various adsorption geometries on single-crystal surfaces, such as Cu(111), Cu(100), and Ni(111), depending on coverage and surface temperature.[1,3,4] It is also found on copper that at high temperatures thermal decomposition of CH_3S leads to evolution of CH_4 and C_2H_6, leaving atomic sulfur.[13] The accumulation of sulfur on the copper surface has been found to act as a poison in the further decomposition of methanethiol into methane and ethane. The sulfur atoms on the surface provide a partially passivated layer for the complete methanethiol decomposition reaction (we call this surface the sulfur-passivated surface).

It has been demonstrated that the TOF-ESDIAD method is useful for imaging different bond positions within a chemisorbed organic molecule that has been strategically labeled with H and D atoms.[14,15] On the basis of ESDIAD patterns measuring H^+ and D^+ ejection from different molecular positions, one can triangulate the structure of the adsorbed molecule, leading to a detailed conformational analysis of the local molecular structure on the adsorption site.

Here we report a study of the adsorption and orientation of methanethiol on the clean Cu(110) surface and the sulfur-passivated Cu(110) surface utilizing temperature-programmed desorption (TPD), low-energy electron diffraction (LEED), and the time-of-flight electron-stimulated desorption ion angular distribution (TOF-ESDIAD) method. An isotopomer of methanethiol, methanethiol-methyl-d_3 (CD_3SH), was used in the TOF-ESDIAD studies. In this paper, we focus on the structural character of methanethiolate on the clean Cu(110) surface and the sulfur-passivated Cu(110) surface, determined from the measured C−D chemical bond direction in methanethiolate-d_3 species. A more detailed study of a mechanism involved in thermal decomposition of methanethiol on the clean Cu(110) surface will follow.[16]

2. Experimental Section

The experiments described in this paper were performed in an ultra-high-vacuum chamber with a base pressure of $< 2 \times 10^{-10}$ Torr. The Cu single crystal, a cylindrical disk 3 mm thick, with a diameter of 10 mm, was oriented to within ±0.22° of the ⟨110⟩ plane. The crystal could be cooled to 80 K using liquid nitrogen, and heated to 900 K by resistive heating.

The copper crystal at 80 K was exposed to methanethiol (99.5%, Aldrich) for temperature-programmed desorption (TPD) and methanethiol-methyl-d_3 (98 at. % D, Isotec Inc.) for ESDIAD studies. Exposure was accomplished using a calibrated microcapillary array beam doser which produced uniform layers while maintaining low background pressure during adsorption.[17] Typically, the adsorbate flux that was employed was in the range

10.1021/jp0302515 CCC: $25.00
Published on Web 09/03/2003

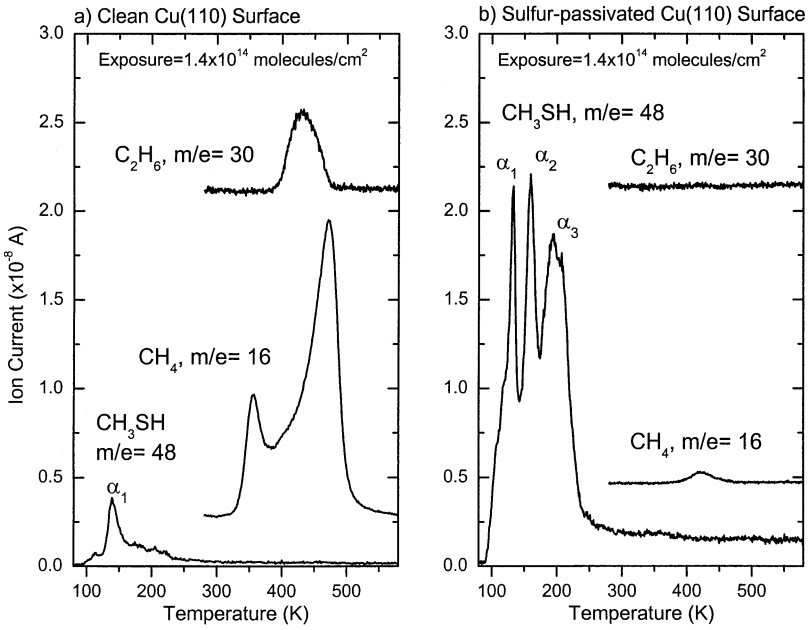

Figure 1. Temperature-programmed desorption spectra of CH_3SH on the clean Cu(110) surface and the sulfur-passivated copper surface.

of 2.0×10^{12} to 1.0×10^{13} molecules cm^{-2} s^{-1}. Desorbing H^+ ions and D^+ ions were produced by electronic stimulation with electron pulses (50 ns width, pulse rate of 10 kHz) each containing 10^4-10^5 electrons with an energy V_e of 180 eV, incident in an ~0.5 mm diameter beam. An accelerating voltage of 25 V was applied to the Cu crystal in all ESDIAD studies to spatially compress the ESDIAD patterns, causing the incident electron energy to be 205 eV. Damage to the adsorbed layer was minimized by using a total effective bombardment time of only ~1 s, in which the total fluence of electrons was only 1.7×10^{12} electrons/cm^2.

The TOF-ESDIAD apparatus, described previously,[18−21] allows for the separation of ESDIAD patterns corresponding to different time-of-flight windows. It is therefore possible to separately measure the ESDIAD patterns of desorbing species having different masses, such as D^+ and H^+.[18,21]

The Cu(110) surface was cleaned by cycles of argon ion bombardment followed by annealing to 900 K. Auger spectroscopy was used to detect impurities on the surface and to assess the accumulation of sulfur atoms on the surface before and after desorption experiments. The level of S impurities on the clean crystal was <0.2 at. % in the depth of Auger sampling.

The ESDIAD apparatus was also used as a low-energy electron diffraction (LEED) apparatus to determine the azimuthal orientation of the Cu(110) crystal in laboratory coordinates and to perform digital LEED measurements for observing the ordered structure of the adsorbate overlayer.

Temperature-programmed desorption (TPD) was carried out using a UTI 100C quadrupole mass spectrometer (QMS) with digital data acquisition with an electronically controlled temperature scan rate dT/dt of 2 K/s, and mass multiplexing was used to monitor the desorbed products. Possible damage to the surface by stray electrons from the QMS ionization source was eliminated by applying a bias potential of −70 V to a grid in front of the QMS source.

3. Results

3.1. Temperature Programmed Desorption and Auger Electron Spectroscopy. Figure 1a shows a TPD spectrum of methanethiol at an exposure of 1.4×10^{14} molecules/cm^2 on a clean Cu(110) surface at 80 K. Methanethiol molecular desorption (α_1, m/e = 48 amu/e) occurred at 140 K. Methane desorption (m/e = 16 amu/e) was observed with two maximum desorption features at 360 and 470 K, and ethane desorption (m/e = 30 amu/e) was observed at 430 K. A substantial amount of hydrogen (H_2) and hydrogen sulfide (H_2S) desorption was not observed in TPD experiments on the clean Cu(110) surface. At higher levels of exposure to methanethiol, the total amount of molecular desorption increased and the desorption temperature decreased slightly. This molecular desorption feature originates from a weakly bound species on the clean surface.

After the first desorption of methanethiol on the clean Cu(110) surface, a substantial amount of sulfur accumulation was detected by Auger electron spectroscopy. In the AES spectrum, although a small amount of carbon also was detected, the carbon intensity did not increase during repeated methanethiol adsorption and desorption experiments. To study the influence of sulfur atom deposition on the adsorption and desorption of methanethiol, repeated doses of methanethiol molecules (1.4×10^{14} molecules/cm^2) were employed without cleaning the surface after each TPD measurement. Following repeated exposure and heating to 673 K, the intensity of the methanethiol molecular desorption peak (α_1) increased and the peak maximum shifted to a lower temperature (130 K). Also, as sulfur accumulated on the surface, two prominent additional desorption peaks appeared at higher temperatures (α_2 and α_3), which have maxima at 160 and 200 K, respectively, as shown in Figure 1b. Finally, the desorption spectrum of methanethiol was unchanged for successive adsorption experiments after seven cycles of exposing and heating, and the relative intensity of the sulfur Auger peak (152 eV) became constant. We call this the fully S-passivated surface. On the fully S-passivated surface, no other gaseous products, such as H_2 and H_2S, were detected during the TPD measurements.

The desorption behavior of methanethiol on the fully passivated Cu(110) surface is quite different from that of methanethiol on a clean Cu(110) surface. Molecular desorption of methanethiol becomes a dominant pathway for thermal desorption on the fully S-passivated surface. The total amount of

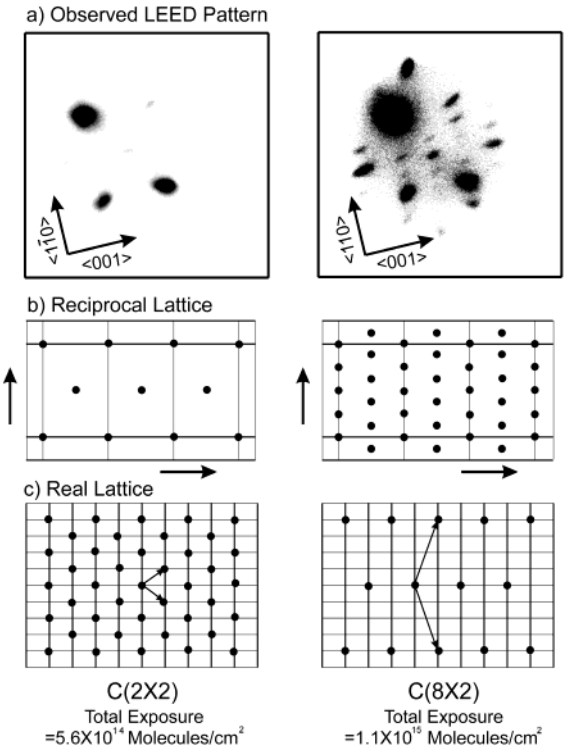

Figure 2. LEED patterns of sulfur on the Cu(110) surface after two levels of passivation.

methane and ethane desorption dramatically decreases on the fully S-passivated surface, and their desorption peaks can hardly be seen in Figure 1b.

Comparing the fully S-passivated surface to the clean Cu(110) surface, we find that the yield of methanethiol increases by more than 1 order of magnitude, and the yield of methane decreases by a factor of 60.

3.2. Low-Energy Electron Diffraction Study of the S-Passivated Cu(110) Surface. LEED experiments were performed to investigate the ordered structures produced by adsorbed methanethiol and by the sulfur atoms released by heating to 673 K. No particular LEED pattern was observed from adsorbed methanethiol at various levels of exposure on the clean Cu(110) surface and on the S-passivated surface. The LEED study for methanethiol on the S-passivated surface could not be carried out in detail because of the interference of the underlying sulfur overlayer structure. To investigate systematically the ordered S-passivated structure, LEED measurements were performed for the overlayer prepared in a manner similar to the repetitive exposure and heating TPD experiments. LEED patterns were measured after each cycle of adsorption and desorption of methanethiol without any cleaning procedure.

Two LEED patterns for the sulfur overlayer during the accumulation of sulfur were distinguished. A $c(2 \times 2)$ LEED pattern was obtained at a relatively low coverage of sulfur on Cu(110) at 80 K. As the coverage increased, a splitting of the ($^1/_2$, $^1/_2$) beam was observed along the $\langle 1\bar{1}0 \rangle$ azimuth. At higher coverage, the $c(2 \times 2)$ LEED pattern converted to a $c(8 \times 2)$ pattern, as shown in Figure 2. After the $c(8 \times 2)$ superstructure was formed on the surface, no further change was observed in the LEED pattern with additional methanethiol exposure, and the ratio of the Auger peak-to-peak height for S at 152 eV and the copper at 920 eV did not change with additional methanethiol exposure and heating. The results from TPD, AES, and LEED experiments therefore indicate that the Cu(110) surface is completely poisoned by the sulfur atoms released by the decomposition of methanethiol and that the sulfur-passivated surface can then provide a passive template for methanethiol adsorption.

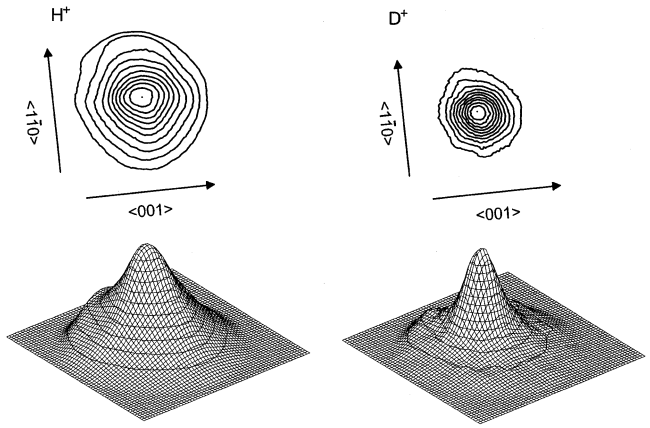

Figure 3. H^+ and D^+ ESDIAD patterns from the CD_3SH isotopomer adsorbed on the clean Cu(110) surface.

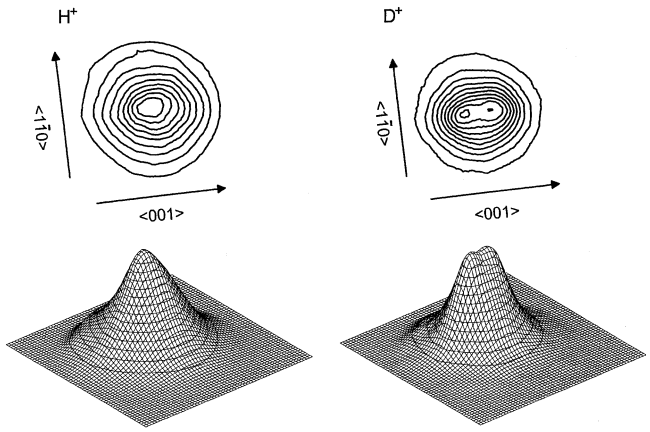

Figure 4. H^+ and D^+ ESDIAD patterns from the CD_3SH isotopomer on the sulfur-passivated Cu(110) surface.

3.3. ESDIAD Study of Methanethiol on the Clean Cu(110) and on the Sulfur-Passivated Cu(110). The methanethiol-methyl-d_3 isotopomer (CD_3SH) was used to monitor separately the ESDIAD patterns for D^+ and H^+ originating from different positions in the adsorbed molecule. According to our observations, isotopic exchange between the deuterium atoms of the methyl group and the hydrogen atoms of the SH group does not occur as a result of the electron bombardment process; therefore, the H^+ ESDIAD pattern is produced from S−H bonds in the SH group, and the D^+ pattern originates from the methyl group of chemisorbed methanethiol. On the clean Cu(110) surface, both the H^+ and D^+ ESDIAD pattern exhibited broad single beams oriented normally to the surface as shown in Figure 3. These H^+ and D^+ ESDIAD patterns did not change after heating to 323 K. On the sulfur-passivated layer, H^+ emission occurred in a broad one-beam normally oriented pattern and the D^+ ESDIAD pattern was split into a two-beam pattern aligned parallel to the $\langle 001 \rangle$ azimuth as shown in Figure 4. This two-beam D^+ pattern became clearer when the surface with adsorbate was heated to 160 K; after the surface had been heated to 250 K, the D^+ pattern disappeared. The angle between the two D^+ beams did not change on heating to 160 K followed by cooling to 80 K. Therefore, the D^+ two-beam ESDIAD pattern on the sulfur-passivated surface originates mainly from the α_3 phase in the TPD spectrum as shown in Figure 1b.

The D^+ ion emission angle with respect to the crystal normal from the methyl group of methanethiol was measured as a

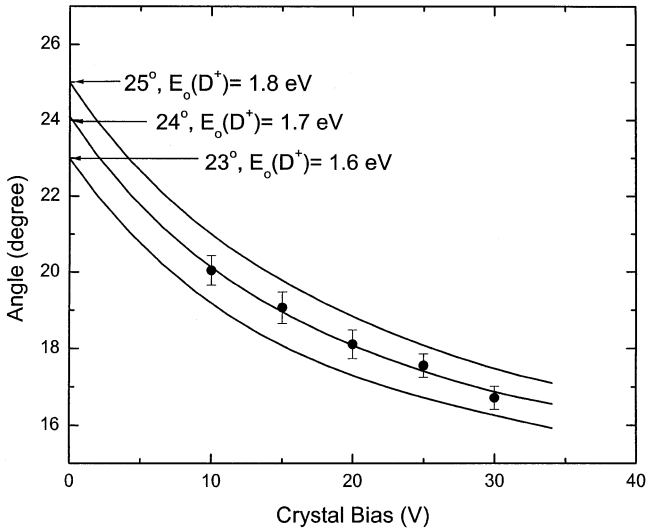

Figure 5. Determination of the D^+ ion emission angle from the adsorbed CD_3SH molecule on the sulfur-passivated surface.

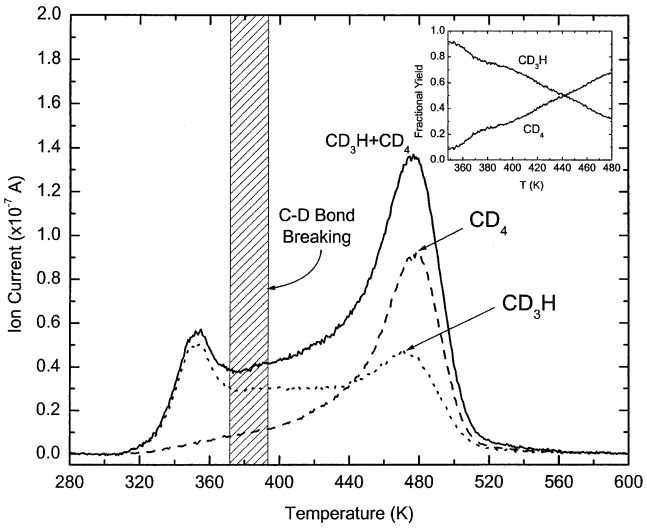

Figure 6. Deconvolution of methane isotopomer desorption from clean Cu(110) using the CD_3SH isotopomer.

function of crystal bias. The D^+ ion emission angle at zero crystal bias was determined by extrapolation of the measured angle to zero crystal bias. To determine the angle between the D^+ beams and the crystal normal at different crystal biases, the ESDIAD patterns were cut along the ⟨001⟩ azimuthal direction and fitted by two Gaussian functions. Angles measured with respect to the normal for various crystal potentials are shown in Figure 5, and the D^+ emission angle at zero crystal bias was determined by the extrapolation of the crystal bias to the zero-field condition using an electrostatic model for the ESDIAD analyzer system.[15] The behavior of the measured D^+ ion ejection angle with respect to crystal bias voltage fits well within the modeled region for a D^+ E_0 energy range between 1.6 and 1.8 eV as obtained from the ion optics computer simulation (solid curves). The field-free ion ejection angle from the crystal normal ranges from 23° to 25° (at zero bias) over the D^+ energy range of 1.6−1.8 eV according to the ion optics simulation results. The best fit for our data involves a D^+ initial kinetic energy E_0 of 1.7 ± 0.1 eV and a zero bias ion ejection angle of 24 ± 1° from the normal. This energy is consistent with the energy calculated from the time-of-flight distribution curve for D^+, which yields a most-probable D^+ kinetic energy of 1.8 ± 0.2 eV.

The final state effects involving the ion image potential and ion reneutralization can influence the zero-field ion desorption angle by distorting the ion trajectories and the angular distributions. Theoretical studies for both the image potential and the reneutralization effect on ion trajectories have been carried out by Madey et al.[22,23] in an effort to obtain the true ion emission angle under the zero-bias condition. Considering both of the final state effects, the angle of ejection of the D^+ ion from the methyl group in methanethiol on the S-passivated Cu(110) surface, derived from the ion optical extrapolation, was corrected to a tilt angle of 26 ± 1° with respect to the surface normal. The angle of emission of the D^+ ion from the CD_3 group of adsorbed methanethiol-d_3 on the sulfur-passivated surface did not exhibit any dependency on surface coverage.

4. Discussion

4.1. Orientation and Thermal Decomposition of Methanethiol on the Clean Cu(110) Surface. The results of the TPD experiments indicate that the methanethiol molecule on the clean Cu(110) surface thermally decomposes to methane and ethane, leaving the sulfur atom on the surface. This result is in agreement with other studies[24,25] with Cu(110) and with the study of Sexton and Nyberg in which HREELS measurements indicate that CH_3SH dissociates on Cu(100).[26]

As shown in Figure 3, both D^+ and H^+ ESDIAD patterns from adsorbed methanethiol on the clean Cu(110) surface consist of one beam centered on the crystal normal. This observation may indicate that both the C−D bond and the S−H bond directions of adsorbed methanethiol are randomly oriented for a randomly oriented CD_3SH molecule adsorbed at 80 K. The summation of the D^+ and H^+ beams from the randomly oriented molecule averages to produce normally oriented patterns. Another interpretation is, however, more likely. In a recent XPS investigation, Lai et al.[13] reported that at low coverage on Cu(110), CH_3SH dissociated mainly to CH_3S(a) and H(a) at 100 K. Therefore, we conclude that the orientation of the C−D bond in CD_3S(a) yields a broad angular distribution of D^+ ions centered on the normal, and that ESDIAD cannot reliably determine the orientation of the S−C bond in adsorbed CD_3S from the D^+ beam directions in this case.

The methanethiolate formed by dissociation of adsorbed methanethiol on Cu(110) thermally decomposes further to form surface sulfur and methyl species as the temperature is increased to 320 K. The formed surface methyl species evolves as methane and ethane by recombination reactions with hydrogen and methyl species in the temperature range of 320−520 K. To understand the methane formation mechanism, a TPD experiment was performed using CD_3SH. By monitoring the ions, CD_3H^+ (m/e = 19) and CD_4^+ (m/e = 20), we can deconvolute the methane desorption peak as shown in Figure 6. We assign the lower-temperature desorption peak to the recombination of a surface methyl group and surface hydrogen and the higher-temperature desorption peak mainly to recombination of the d_3-methyl group and deuterium from dissociation of the C−D bond. The inset of Figure 6 shows clearly that the mole fraction of CD_4 increases with increasing temperature as CD_3SH decomposes and produces methane by two kinetic routes. As detected by AES measurements after annealing, some atomic carbon remains on the surface after thermal decomposition of methanethiol from the dehydrogenation of the surface methyl species.

On the basis of TPD and TOF-ESDIAD experiments, we categorize the following possible reactions related to the thermal decomposition of methanethiol on the clean Cu(110) surface:

(1) CH_3S-H bond breaking around 80−200 K, (2) CH_3-S bond breaking below 250−320 K, (3) CH_2-H bond breaking near 370−380 K, (4) $CH_3\cdots CH_3$ recombination around 400−480 K, and (5) $CH_3\cdots H$ recombination around 320−520 K.

In contrast to another study,[13] we did not observe the evolution of hydrogen as a product of methanethiol thermal decomposition; hydrogen is commonly observed in thermal decomposition of hydrocarbons on metal surfaces. One explanation for the lack of observed H_2 evolution is that hydrogen is converted to methane. In addition, traces of hydrogen may desorb but are masked by the background hydrogen signal.

4.2. Cu(110)−Sulfur Surface. We observed two LEED patterns, $c(2 \times 2)$ and $c(8 \times 2)$, as the sulfur coverage increases. At low sulfur coverages, the $c(2 \times 2)$ structure was observed. The $c(2 \times 2)$ pattern converted to the $c(8 \times 2)$ structure once sulfur saturation was reached. This observation of LEED patterns for the sulfur-covered surface structure on Cu(110) is consistent with other studies except we did not observe either the $p(3 \times 2)$ or the $p(5 \times 2)$ phase.[27−29] These results suggest that sulfur reconstructs the surface, producing a long-range periodicity at high coverages.

So far, various sulfur adsorption models have been suggested in previous studies of sulfur on the Cu(110) surface prepared by exposing it to hydrogen sulfide using LEED, SEXAFS, and STM. In these studies, it was proposed either that the sulfur layer was planar on the underlying surface copper layer or that the sulfur atoms might not be coplanar because of different adsorption sites. In a recent study, an alternative model involving surface buckling has been suggested by Carley et al.,[25] who found the $c(8 \times 2)$ structure is proposed to be a combination of the $p(5 \times 2)$ and $p(3 \times 2)$ structures and sulfur is chemisorbed preferentially at the 2-fold hollow copper site. However, this model was not consistent with the results of a SEXAFS study, in which all different LEED structures have the same Cu−S bond distance.[30]

4.3. Methanethiol Adsorption on the Sulfur-Passivated Cu(110) Surface. *4.3.1. Formation of Methanethiolate Species on the Sulfur-Passivated Cu(110) Surface.* The results of the TPD experiments on the sulfur-passivated surface indicate that there are at least three desorption states for methanethiol as shown in Figure 1. The desorption peak at 130 K (α_1) on the sulfur-passivated surface desorbs at a temperature similar to that of the most weakly held undissociated species on the clean Cu(110). The new desorption peaks (α_2 and α_3) develop at 160 and 200 K, respectively, temperatures which are 30 and 70 K higher, respectively, than the desorption temperature of the most weakly held species. There are three possible origins for these two new desorption features characteristic of CH_3SH adsorption on S-passivated Cu(110): (1) the stabilization of molecular methanethiol by hydrogen bond formation with the sulfur overlayer, (2) the chemisorbed methanethiol species which is more strongly covalently bound to a S underlayer then to a clean Cu surface, or (3) recombination of surface hydrogen with methanethiolate, formed by the dissociation of methanethiol.

Two properties of the CD_3SH molecule are evident when comparing the TPD experiment with the ESDIAD experiment for CD_3SH on the S-passivated surface.

(1) An inclined C−D bond is observed by ESDIAD, where the S−H bond direction is not inclined to the normal (Figure 4).

(2) Molecular CD_3SH desorbs from the S-passivated surface in several kinetic processes below 250 K (Figure 1b).

These results are consistent with each other if we postulate that CD_3SH adsorbs on the S-passivated surface as CD_3S and H species at 80 K, and that these fragments recombine to produce CD_3SH during thermal desorption.

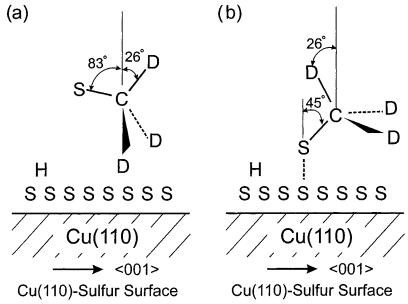

Figure 7. Possible structures for methanethiolate on the sulfur-passivated Cu(110) surface. We believe that structure a is unlikely.

The bonding of CD_3S to an underlying S-passivated surface by the formation of a disulfide bond (CD_3S-S) has been proposed in many analogous system such as ethanethiol on $MoS_2(0001)$,[31] benzenethiol on S-covered Mo(110),[32] and methanethiol on the sulfide W(211) surface.[33]

4.3.2. Orientation of Methanethiolate Species on the Sulfur-Passivated Surface. The orientation of C−S bond axis of methanethiolate on the sulfur-passivated Cu(110) surface was determined from the C−D bond direction in the methyl group using the knowledge of the molecular structure of methanethiol in the gas phase. One can expect various ESDIAD patterns from the methyl group for different geometries of the methyl group with respect to the surface normal. For example, a ring pattern will be expected for a rotating methyl group in the case in which the rotation axis is perpendicular to the surface. Such a pattern has been seen for the methyl group in the acetate species on Cu(110).[34] Also, a tilted rotating methyl group has been observed from another species terminated with a CH_3 group.[15] The observation of a two-beam D^+ pattern indicates that the methyl group of CD_3S on the sulfur-passivated surface does not freely rotate at 80 K and that all three deuterium atoms cannot be seen by ESDIAD. Figure 7 shows two possible structures for the CD_3S species on the S-passivated Cu(110) surface. Both structures involve a C−D bond directed 26° off normal along the ⟨001⟩ azimuth. In Figure 7a, two D atoms are directed downward and the S atom is far from the surface of S atoms. This structure is unlikely on energetic grounds. In Figure 7b, the S atom of CD_3S is relatively strongly bound to the underlying S layer. This tilted structure projects the CD_3 group upward, and the rotation of the CD_3 group may be prevented by weak interaction of the S···D group with the underlying sulfur layer and by the rotational barrier of the methyl group itself [in the gas phase ($E_{rot} = 30$ meV) which corresponds to a mean thermal energy of ∼350 K],[35] indicating that CD_3 rotation is unexpected at 80 K.

We also found the configuration of methanethiolate on the sulfur-passivated surface did not exhibit a coverage dependency, as judged from the constant nature of the two-beam D^+ pattern with increasing coverage. This indicates that the formation of the oriented structure of methanethiolate (Figure 7b) is governed by the interaction between the methanethiolate sulfur and the passivated sulfur layer.

4.4. Comparison of the Methanethiolate Configuration on the Clean Cu(110) Surface with the Configuration on the Sulfur-Passivated Surface. In Figure 8, we display the configurations of methanethiolate both on the clean Cu(110) surface and on the sulfur-passivated surface which were obtained from the ESDIAD studies. Judging from the normally oriented D^+ beam from CD_3S on the clean Cu(110) as shown in Figure 3,

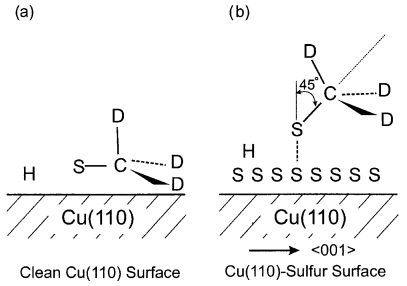

Figure 8. Comparison of methanethiolate configurations on (a) clean and (b) S-passivated Cu(110).

we propose that methanethiolate is oriented in a lying-down manner on the clean Cu(110) surface. This configuration, shown in Figure 8a, presents a C−D bond which is near the normal direction on average. It involves pinning both the C atom and the S atom to the clean Cu(110) surface. On the sulfur-passivated surface, the C−S bond of the methanethiolate molecule is aligned parallel to the ⟨001⟩ azimuth and the molecular axis (C−S bond axis) is tilted 45° away from the surface normal.

From this point of view, the Cu(110) surface is highly reactive for methanethiol molecules and may be a poor substrate for formation of methanethiolate SAM structures. The sulfur-passivated copper surface on the other hand would be a better substrate than the clean copper surface for preparing a self-assembled layer of alkanethiolate.

Our results for adsorption and thermal decomposition of methanethiol provide information about the structure and thermal stability of alkanethiols on the copper surface. Although we prepared a methanethiolate layer on the surface under UHV conditions, which differs from a SAM prepared in solution, we believe that this study provides deeper insights into the details of the chemistry and surface bonding in self-assembly.

5. Summary

The following results have been obtained for the interaction of methanethiol with the clean Cu(110) surface and with the sulfur-passivated Cu(110) surface.

(1) On the clean Cu(110) surface, methanethiol decomposes, leaving the sulfur atoms on the surface. Both CH_4 and C_2H_6 are formed above 320 K. The decomposition reaction is passivated by accumulated sulfur.

(2) On the clean surface, the ESDIAD patterns of H^+ and D^+ are normally oriented. This suggests that the orientation of methanethiolate involves a structure in which the CD_3 group and the S atom are pinned in a general way to the Cu(110) surface. An azimuthal orientation of the C−S bond is not observed.

(3) LEED, AES, and TPD studies show that the sulfur-passivated copper surface is chemically stable and forms a template for the ordered adsorption of methanethiol.

(4) The tilt angle and azimuthal angle of the C−S bond axis of methanethiolate on the sulfur-passivated Cu(110) surface have been determined by TOF-ESDIAD. The C−S bond in methanethiolate on the sulfur-passivated surface is aligned parallel to the ⟨001⟩ azimuthal direction. The C−S bond of methanethiolate tilts 45° with respect to surface normal in the ⟨001⟩ azimuth.

(5) No coverage dependency for C−D bond orientation in the methanethiolate layer on S-passivated Cu(110) was observed. This indicates that the structure of methanethiolate on the sulfur-passivated surface is influenced by a strong interaction between the sulfur layer and the molecule rather than by adsorbate−adsorbate interactions.

Acknowledgment. We acknowledge with thanks the support of this work by the Department of Energy, Office of Basic Energy Sciences.

References and Notes

(1) Kariapper, M. S.; Fisher, C.; Woodruff, D. P.; Cowie, B. C. C.; Jones, R. G. *J. Phys. Condens. Matter* **2000**, *12*, 2153.

(2) Kariapper, M. S.; Grom, G. F.; Jackson, G. J.; MacConville, C. F.; Woodruff, D. P. *J. Phys. Condens. Matter* **1998**, *10*, 8661.

(3) Jackson, G. J.; Woodruff, D. P.; Jones, R. G.; Singh, N. K.; Chan, A. S. Y.; Cowie, B. C. C.; Formoso, V. *Phys. Rev. Lett.* **2000**, *84*, 119.

(4) Mullins, D. R.; Huntley, D. R.; Yang, T.; Saldin, D. K.; Tysoe, W. T. *Surf. Sci.* **1997**, *380*, 468.

(5) Kondoh, H.; Nozoye, H. *J. Phys. Chem. B* **1998**, *102*, 2367.

(6) Chang, S. C.; Chao, I.; Tao, Y.-T. *J. Am. Chem. Soc.* **1994**, *116*, 6792.

(7) Walczak, M. M.; Chung, C.; Stole, S. M.; Widrig, C. A.; Porter, M. D. *J. Am. Chem. Soc.* **1991**, *113*, 2370.

(8) Heister, K.; Rong, H.-T.; Buck, M.; Zharnikov, M.; Grunze, M.; Johansson, L. S. O. *J. Phys. Chem. B* **2001**, *105*, 6888.

(9) Laibinis, P. E.; Whitesides, G. M.; Allara, D. L.; Tao, Y.-T.; Parikh, A. N.; Nuzzo, R. G. *J. Am. Chem. Soc.* **1991**, *113*, 7152.

(10) Kühnle, A.; Vollmer, S.; Linderoth, T. R.; Witte, G.; Wöll, C.; Besenbacher, F. *Langmuir* **2002**, *18*, 5558.

(11) Frey, S.; Stadler, V.; Keister, K.; Eck, W.; Zarnikov, M.; Grunze, M.; Zeysing, B.; Terfort, A. *Langmuir* **2001**, *17*, 2408.

(12) Lee, J.-G.; Lee, J.; Yates, J. T., Jr., submitted.

(13) Lai, Y.-H.; Yeh, C. T.; Cheng, S.-H.; Liao, P.; Hung, W.-H. *J. Phys. Chem. B* **2002**, *106*, 5438.

(14) Lee, J.-G.; Ahner, J.; Maksymovych, P.; Yates, J. T., Jr. *Chem. Phys. Lett.* **2001**, *340*, 21.

(15) Lee, J.-G.; Ahner, J.; Yates, J. T., Jr. *J. Am. Chem. Soc.* **2002**, *124*, 2772.

(16) Lee, J.-G.; Lee, J.; Yates, J. T., Jr., submitted to *J. Phys. Chem. B.*

(17) Yates, J. T., Jr. *Experimental Innovations in Surface Science*; AIP Press and Springer-Verlag: New York, 1998.

(18) Ahner, J.; Mocuta, D.; Yates, J. T., Jr. *J. Vac. Sci. Technol., A* **1999**, *17*, 2333.

(19) Mocuta, D.; Ahner, J.; Yates, J. T., Jr. *Surf. Sci.* **1997**, *383*, 299.

(20) Mocuta, D.; Ahner, J.; Yates, J. T., Jr. *Surf. Sci.* **1997**, *390*, 126.

(21) Ahner, J.; Mocuta, D.; Yates, J. T., Jr. *Surf. Sci.* **1997**, *390*, 11.

(22) Mišković, Z.; Vukanić, J.; Madey, T. E. *Surf. Sci.* **1986**, *169*, 405−413.

(23) Mišković, Z.; Vukanić, J.; Madey, T. E. *Surf. Sci.* **1984**, *141*, 285−300.

(24) Carley, A. F.; Davies, P. R.; Jones, R. V.; Harikumar, K. R.; Roberts, M. W. *Surf. Sci.* **2001**, *490*, L585.

(25) Carley, A. F.; Davies, P. R.; Jones, R. V.; Harikumar, K. R.; Kulkarni, G. U.; Roberts, M. W. *Surf. Sci.* **2000**, *447*, 39.

(26) Sexton, B. A.; Nyberg, G. L. *Surf. Sci.* **1986**, *165*, 251.

(27) Boulliard, J. C.; Sotto, M. P. *Surf. Sci.* **1989**, *217*, 38.

(28) Maurice, V.; Oudar, J.; Huber, M. *Surf. Sci.* **1987**, *187*, 312.

(29) Bonzel, H. P. *Surf. Sci.* **1971**, *27*, 387.

(30) Atrei, A.; Johnson, A. L.; King, D. A. *Surf. Sci.* **1991**, *254*, 65.

(31) Peterson, S. L.; Schulz, K. H. *Langmuir* **1996**, *12*, 941.

(32) Weldon, M. K.; Napier, M. E.; Wiegand, B. C.; Friend, C. M.; Uvdal, P. *J. Am. Chem. Soc.* **1994**, *116*, 8328.

(33) Benziger, J. B.; Preston, R. E. *J. Phys. Chem.* **1985**, *89*, 5002.

(34) Lee, J.-G.; Ahner, J.; Mocuta, D.; Denev, S.; Yates, J. T., Jr. *J. Chem. Phys.* **2000**, *112*, 3351.

(35) Kilb, R. W. *J. Chem. Phys.* **1955**, *23*, 1736.